ELSEVIER

Journal of Non-Crystalline Solids 235–237 (1998) 34–40

JOURNAL OF NON-CRYSTALLINE SOLIDS

Kinetic heterogeneities and non-linear rheology of highly supercooled liquids

Akira Onuki *, Ryoichi Yamamoto

Department of Physics, Kyoto University, Kyoto 606 01, Japan

Abstract

Supercooled liquids with soft-core potentials are studied via molecular dynamics simulations in two and three dimensions in quiescent and sheared conditions. We demonstrate that bond breakage events among particle pairs occur collectively in clusters. The average life time, $\tau_b(\dot\gamma)$, of bonds tends to the α relaxation time, τ_α, for weak shear, $\dot\gamma \ll 1/\tau_\alpha$, and decreases as $1/\dot\gamma$ for strong shear, $\dot\gamma \gg 1/\tau_\alpha$. The structure factor, $S_b(q)$, of the broken bonds may be fitted to the Ornstein–Zernike form. The correlation length, ξ, is uniquely expressed in terms of $\tau_b(\dot\gamma)$ as $\xi \sim \tau_b(\dot\gamma)^{1/4}$ in two dimensions and $\xi \sim \tau_b(\dot\gamma)^{1/2}$ in three dimensions for any T and $\dot\gamma$ in glassy states. The viscosity is of order $\tau_b(\dot\gamma)$ for any $\dot\gamma$, so the shear stress tends to a limiting stress for $\dot\gamma\tau_\alpha \gg 1$.

1. Introduction

Extensive efforts have recently been made to study structural relaxations in glass-forming liquids and polymers [1,2]. In particular, the structural or α relaxation time, τ_α, becomes exceedingly long. As a first analytic scheme the mode coupling theory [3,4] describes thermal disordering of local crystalline structures and predicts onset of glassy slowing down, but it predicts no long range correlations. As the temperature is further lowered, however, we naturally expect that dynamics in glasses should be cooperative, involving many molecules, owing to configuration restrictions [5–8]. Adam and Gibbs [5] speculated that particle motions over the interparticle distance or the potential barrier can take place only collectively in *cooperatively rearranging regions* (CRR) and such regions have a *minimum* size which grows as temperature is decreased. Our recent MD simulation in two dimensions [9] has demonstrated that such CRR may be identified as *weakly bonded* regions with various sizes. Their *maximum* size, ξ, grows as $\tau_\alpha^{1/4}$ and those smaller than ξ are insensitive to T, so they are analogous to the critical fluctuations in Ising systems.

Most previous papers so far are concerned with near-equilibrium properties such as relaxations of the density time-correlation functions or dielectric response. The aim of this paper is to demonstrate the presence of a new problem in far-from-equilibrium properties of glassy states. Here we are interested in nonlinear response when the shear rate, $\dot\gamma$, exceeds $1/\tau_\alpha$. Such nonlinear regimes have been studied in various complex fluids [10].

In their experiment, Simmons et al. [11] found that the viscosity, $\eta(\dot\gamma) \equiv \sigma_{xy}/\dot\gamma$, exhibits marked shear-thinning behavior, $\eta(\dot\gamma) \cong \eta(0)/[1 + \dot\gamma\tau_\eta]$, in soda lime–silica glasses in steady states under shear. Here we expect $\tau_\eta \sim \tau_\alpha$ [12]. This remarkably

* Corresponding author. Tel.: 81 75 7533743; fax: 81 75 7533819; e-mail: onuki@ton.scphys.kyoto-u.ac.jp.

0022-3093/98/$19.00
PII: S0022-3093(98)00558-4

simple result indicates that the shear stress approaches a limiting stress, $\sigma_{\rm lim} = \eta(0)/\tau_\eta$, which is of the order of the shear modulus insensitive to T, for $\dot\gamma \gg 1/\tau_\alpha$. Moreover, after application of shear, they also observed overshoots of the shear stress before approach to steady states. Very recently we have applied shear in our MD simulation of a two-dimensional binary mixture [13] to have reproduced shear-thinning behavior in agreement with the experiment. This paper summarizes our simulation results in two dimensions [9,13] and presents new results in three dimensions.

2. MD simulations

We perform MD simulations in two dimensions (2D) and three dimensions (3D) on binary mixtures composed of two different atomic species, 1 and 2, with $N_1 = N_2 = 5000$ particles. Parameters chosen are mostly common in 2D and 3D. They interact via the soft-core potential, $v_{\alpha\beta}(r) = \epsilon(\sigma_{\alpha\beta}/r)^{12}$, with $\sigma_{\alpha\beta} = (\sigma_\alpha + \sigma_\beta)/2$, where r is the distance between two particles and $\alpha, \beta = 1, 2$ [14,15]. The interaction is truncated at $r = 4.5\sigma_1$ in 2D and $r = 3\sigma_1$ in 3D. The leapfrog algorithm is adopted to solve the differential equations with a time step of $0.005\tau_0$. The space and time are measured in units of σ_1 and $\tau_0 = (m_1\sigma_1^2/\epsilon)^{1/2}$. The mass ratio is $m_2/m_1 = 2$, while the size ratio is $\sigma_2/\sigma_1 = 1.4$ in 2D and $\sigma_2/\sigma_1 = 1.2$ in 3D. Our two component systems remain amorphous at low temperatures, because the difference of the particle sizes prevents crystallization.

The average density is fixed at $n = 0.8/\sigma_1^d$. This density is so high such that all the pair distribution functions $g_{\alpha\beta}(r)$ have a sharp peak at $r \cong \sigma_{\alpha\beta}$ as shown in Fig. 1 for 2D. Then our binary mixtures may be fairly mapped onto one-component fluids with the soft-core potential [16,17], whose thermodynamic states are characterized by a single parameter,

$$\Gamma_{\rm eff} = n(\epsilon/k_{\rm B}T)^{d/12}\sum_{\alpha,\beta} x_\alpha x_\beta \sigma_{\alpha\beta}^d. \tag{1}$$

Here x_1 and x_2 are the compositions of the two components and are 1/2 in our case. Data are taken at $\Gamma_{\rm eff} = 1.0$, 1.1, 1.2, 1.3, 1.4 for 2D and

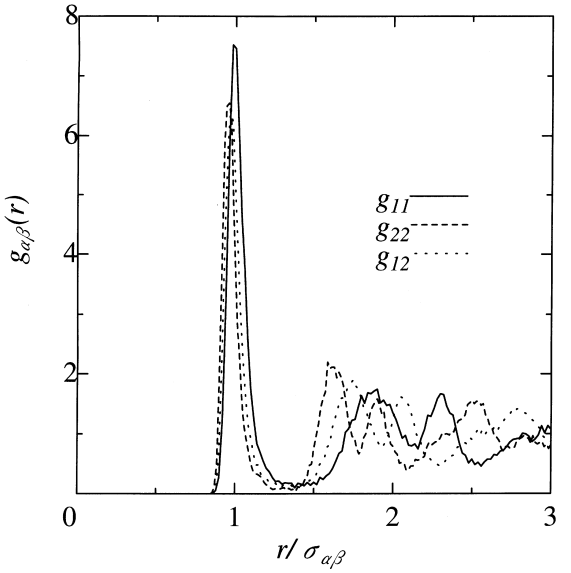

Fig. 1. The pair correlation functions $g_{\alpha\beta}(r)$ at $\Gamma_{\rm eff} = 1.4$ in 2D as functions of $r/\sigma_{\alpha\beta}$.

1.15, 1.30, 1.40, 1.45, 1.5 for 3D. The corresponding temperature is 2.54, 1.43, 0.850, 0.526, 0.337 in 2D and is 0.772, 0.473, 0.352, 0.306, 0.267, 0.234 in 3D, respectively, in units of $\epsilon/k_{\rm B}$. We detect no enhancement of the fluctuations in the density difference $n_1 - n_2$ at any wave numbers. The system is also confirmed to be highly incompressible in the sense that the volume fraction $\sigma_1^d n_1 + \sigma_2^d n_2$ exhibits very small fluctuations at wave numbers smaller than the first peak position.

The system is quiescent for $t < 0$ and is sheared for $t > 0$. To this end we add the average velocity, $\dot\gamma y$, to the velocities of all the particles in the x direction at $t = 0$ and afterwards maintain the shear flow by using the Lee–Edwards boundary condition [18,19]. Then steady states are realized after a transient time. In our case shear flow serves to destroy glassy structures and produces no long range structure. The temperature is kept constant using the Gaussian constraint thermostat [18,19].

3. Quiescent states

For each atomic configuration given at time t_0, a pair of atoms i and j is considered to be bonded if

$$r_{ij}(t_0) = |\boldsymbol{r}_i(t_0) - \boldsymbol{r}_j(t_0)| \leqslant A_1\sigma_{\alpha\beta}, \tag{2}$$

where i and j belong to the species α and β, respectively, and $\sigma_{\alpha\beta} = \frac{1}{2}(\sigma_\alpha + \sigma_\beta)$. We have set $A_1 = 1.1$ for 2D and 1.5 for 3D. However, our bond definition is insensitive to A_1 as long as it is somewhat larger than 1 and smaller than the second peak distances divided by $\sigma_{\alpha\beta}$. This is because all the pair distribution functions $g_{\alpha\beta}(r)$ have a sharp peak at $r \cong \sigma_{\alpha\beta}$ as shown in Fig. 1. The bonds thus defined have lengths close to $\sigma_{\alpha\beta}$ and the polygons composed of the bonds are mostly triangles as shown in Fig. 2. After a lapse of time Δt a pair is regarded to have been broken if

$$r_{ij}(t_0 + \Delta t) > A_2\sigma_{\alpha\beta} \tag{3}$$

with $A_2 = 1.6$ for 2D and 1.5 for 3D. This definition of bond breakage is also insensitive to A_2. Then the number of the surviving bonds is found to decrease exponentially as $\exp(-\Delta t/\tau_b(0))$, which has been confirmed for $\Delta t \lesssim \tau_b(0)$ for each T. The bond breakage time, $\tau_b(0)$, is displayed in Fig. 3 as a function of the inverse temperature. It is of the order of the α relaxation time, τ_α [9]. To be precise, however, the relaxation is better described by the stretched exponential form $\exp[-(\Delta t/\tau_b(0))^a]$ on longer time scales particularly in 3D, where the exponent a decreases with lowering T from 1 down to 0.6 at the lowest T.

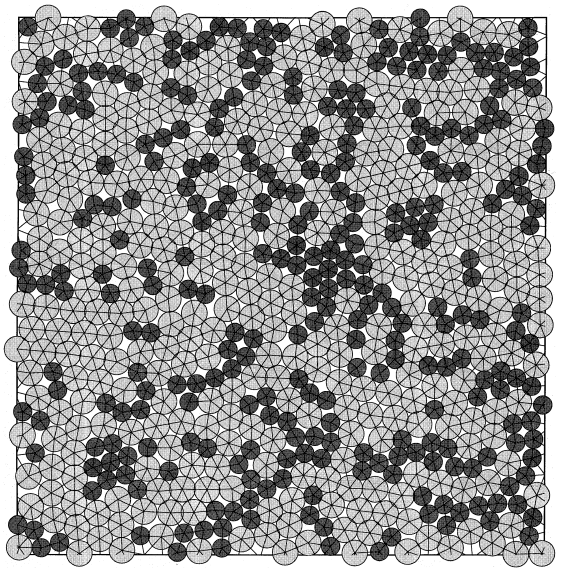

Fig. 2. Bonds defined at a given time at $\Gamma_{\rm eff} = 1.4$ in 2D. Their lengths are mostly close to $\sigma_{\alpha\beta}$. The diameters of the circles here are equal to σ_α. One sixteenth of the total system is shown.

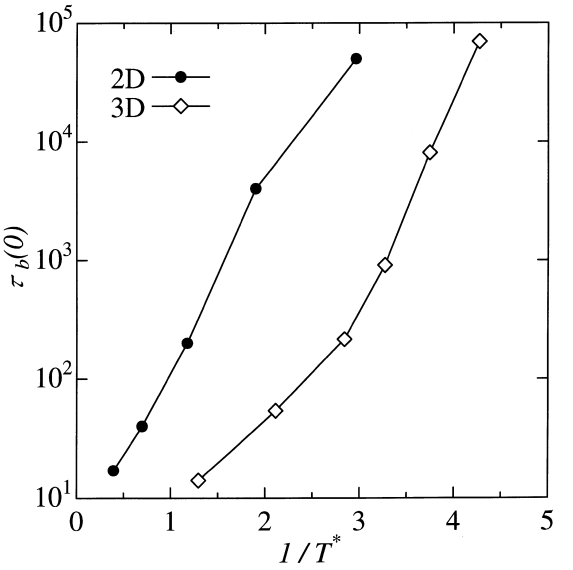

Fig. 3. Temperature dependence of the bond breakage time $\tau_b(0)$ (●) in 2D and (◇) in 3D, where $T^* = k_B T/\epsilon$.

Fig. 4 displays the bonds broken within the time interval, $[t_0, t_0 + 0.05\tau_b]$, at $\Gamma_{\rm eff} = 1.0$ and 1.3 in 2D. The center positions $\boldsymbol{R}_{ij} = (\frac{1}{2}\boldsymbol{r}_i(t_0) + \boldsymbol{r}_j(t_0))$ at the initial time, t_0, of the pairs broken within the time interval are depicted here. For the glassy case $\Gamma_{\rm eff} = 1.3$, the broken bonds form clusters with various sizes and are heterogeneous, whereas for the liquid case $\Gamma_{\rm eff} = 1$, the inhomogeneity is much smaller. As can be clearly seen, elementary processes of bond breakage are string-like jump motions involving several particles even in liquid states, due to the high density of our system. Remarkably, such strings *aggregate* in glassy states. Fig. 5 shows the broken bonds in two consecutive time intervals, $[t_0, t_0 + 0.1\tau_b]$ and $[t_0 + 0.1\tau_b, t_0 + 0.2\tau_b]$, at $\Gamma_{\rm eff} = 1.4$ in 2D. The initial times at which the bonds are defined are t_0 and $t_0 + 0.1\tau_b$, respectively. We can see that the clusters of broken bonds in the two time intervals mostly overlap or are adjacent to each other. Therefore, *weakly bonded regions* or *relatively active regions* migrate in space on the time scale of τ_b.

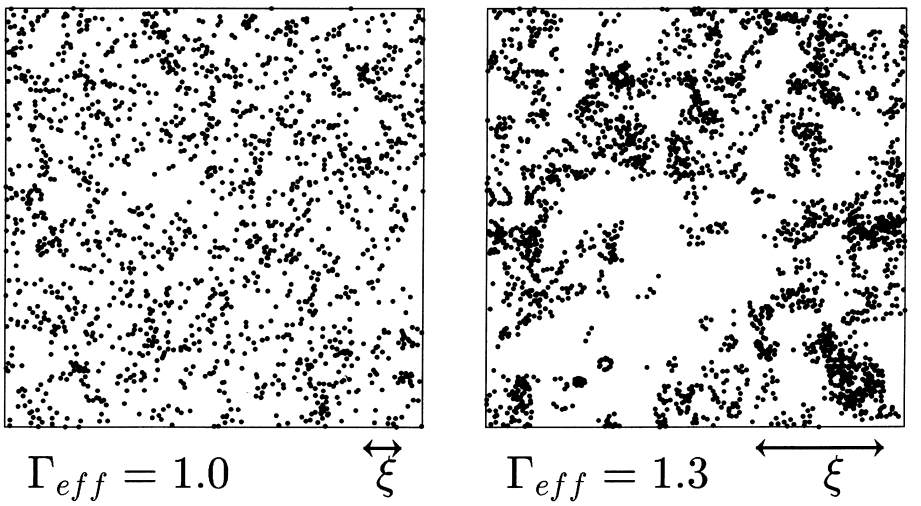

Fig. 4. Snapshots of the broken bonds at $\Gamma_{\rm eff} = 1.0$ and 1.3 in 2D. The time interval is $0.05\tau_{\rm b}(0)$, so 5% of the initial bonds are broken here. The arrows indicate ξ.

We next calculate the structure factor, $S_{\rm b}(q)$, (Fig. 6) of the broken bonds defined by

$$S_{\rm b}(q) = N_{\rm b}^{-1}\left\langle \left| \sum \exp(i\boldsymbol{q}\cdot\boldsymbol{R}_{ij}) \right|^2 \right\rangle. \quad (4)$$

The summation is over the broken pairs, $N_{\rm b}$ is the total number of the broken bonds, and the angular average over the direction of the wave vector is taken. Furthermore, taking the averages of 4–20 sequential configurations, we find that $S_{\rm b}(q)$ can be approximated by the Ornstein–Zernike form,

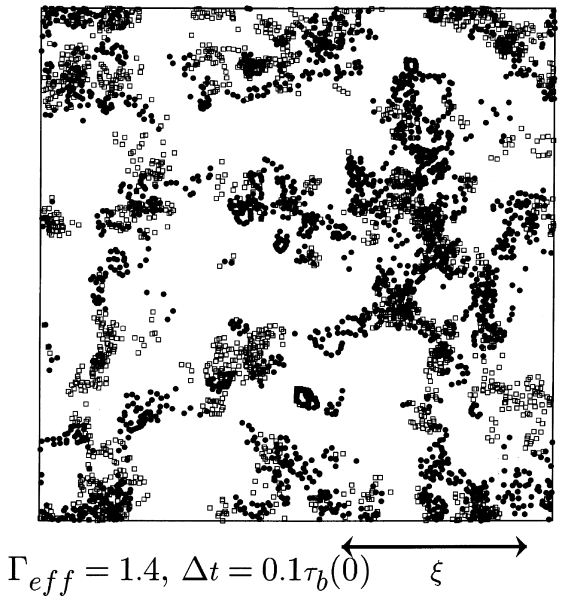

Fig. 5. Broken bonds in two consecutive time intervals, $[t_0, t_0 + 0.1\tau_{\rm b}]$ (□) and $[t_0 + 0.1\tau_{\rm b}, t_0 + 0.2\tau_{\rm b}]$ (●), at $\Gamma_{\rm eff} = 1.4$ in 2D. The arrow indicates ξ.

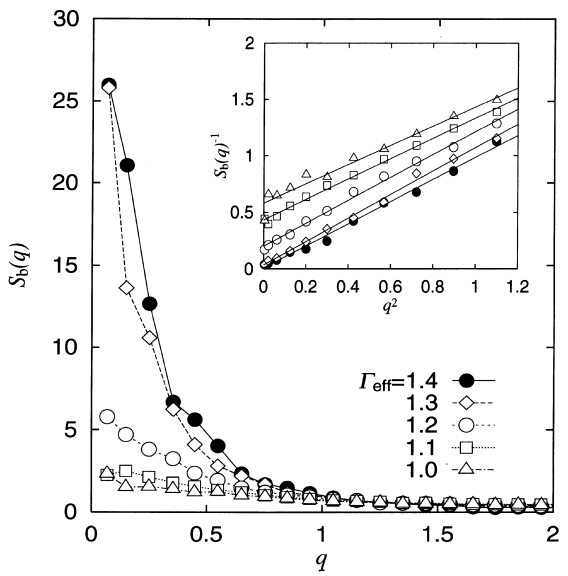

Fig. 6. $S_{\rm b}(q)$ of the broken bond density in 2D. The insert shows $1/S_{\rm b}(q)$ vs q^2, from which ξ^{-2} is determined.

$$S_b(q) = S_b(0)/[1 + \xi^2 q^2]. \quad (5)$$

Interestingly, $S_b(0) \propto \xi^2$ and the large q behavior of $S_b(q)$ is insensitive to T as in Ising systems near the critical point.

We have confirmed that the correlation length, ξ, is insensitive to the width of the time interval, Δt, as long as it is considerably shorter than $\tau_b(0)$ [9].

4. Sheared states

Under shear the bond breakage rate simply consists of the thermal breakage rate and a shear-induced breakage rate as

$$1/\tau_b(\dot\gamma) \cong 1/\tau_b(0) + A_b\dot\gamma, \quad (6)$$

where $A_b = 0.57$ in 2D and 0.80 in 3D, and $\tau_b(0) \sim \tau_\alpha$. Thus, for strong shear $\dot\gamma\tau_\alpha \gg 1$, disordering of glassy structures is achieved by shear-induced jump motions. In our systems, furthermore, the structure factor $S_b(q)$ of the broken bonds is only weakly dependent on the direction of the wave vector $\boldsymbol{q}$ and may be fitted to the Ornstein–Zernike form. As shown in Figs. 7 and 8, $\xi(\dot\gamma)$ is uniquely determined by $\tau_b(\dot\gamma)$ only as

$$\xi(\dot\gamma) \sim \tau_b(\dot\gamma)^{1/z} \quad (7)$$

for any $\Gamma_{\rm eff}$ and $\dot\gamma$ used in our simulations. The dynamic exponent z is 4 in 2D and 2 in 3D. Notice that the data points at the largest ξ are those at zero shear for each $\Gamma_{\rm eff}$. This relation suggests that the steady states may be characterized by a single parameter, say ξ, and that each steady state in the non-Newtonian regime may be mapped onto a quiescent state at a higher temperature with the same ξ.

We have also found that the viscosity is determined solely by $\tau_b(\dot\gamma)$ as

$$\eta(\dot\gamma) \cong A_\eta\tau_b(\dot\gamma) + \eta_B \cong A_\eta\tau_b(0)/[1 + A_b\dot\gamma\tau_b(0)] + \eta_B, \quad (8)$$

where A_η and η_B are 0.34 and 6.25 in 2D, and 0.24 and 2.2 in 3D, respectively. The limiting shear stress $\sigma_{\rm lim} = A_\eta/A_b$ is realizable for $1/\tau_\alpha \ll \dot\gamma \ll \sigma_{\rm min}/\eta_B$, and is 0.59 in 2D and 0.30 in 3D in units of ϵ/σ_1^2. Figs. 9 and 10 show that the ratio $(\eta(\dot\gamma) - \eta_B)/(\eta(0) - \eta_B)$ can be fitted to the universal curve $1/(1 + A_b x)$ with $x = \dot\gamma\tau_b(0)$ independently of $\Gamma_{\rm eff}$.

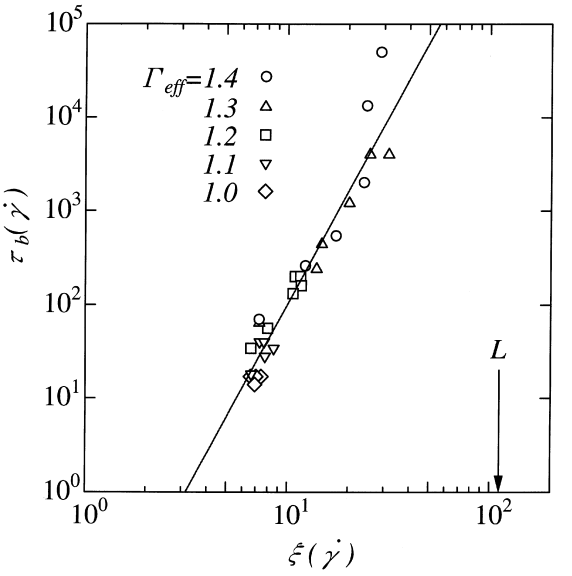

Fig. 7. Universal relation between $\xi(\dot\gamma)$ and $\tau_b(\dot\gamma)$ in 2D. The line of the slope 1/4 is a viewing guide.

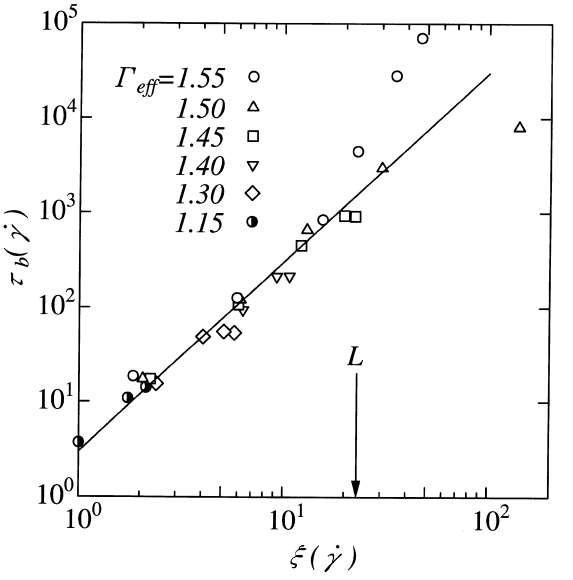

Fig. 8. Universal relation between $\xi(\dot\gamma)$ and $\tau_b(\dot\gamma)$ in 3D. The line of the slope 1/2 is a viewing guide.

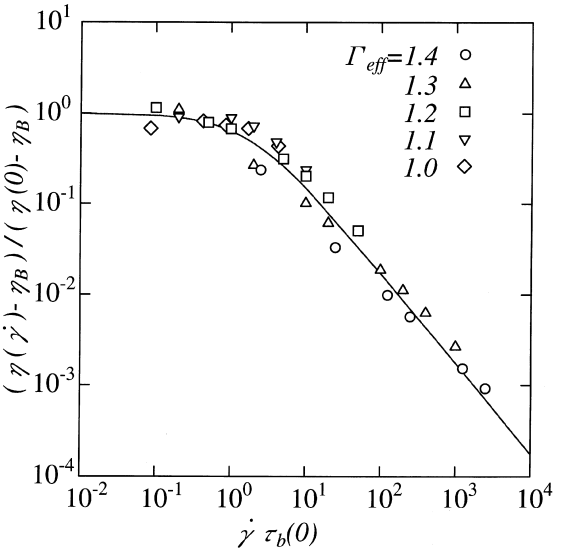

Fig. 9. $(\eta(\dot\gamma)-\eta_B)/(\eta(0)-\eta_B)$ versus $\dot\gamma\tau_b(0)$ in 2D.

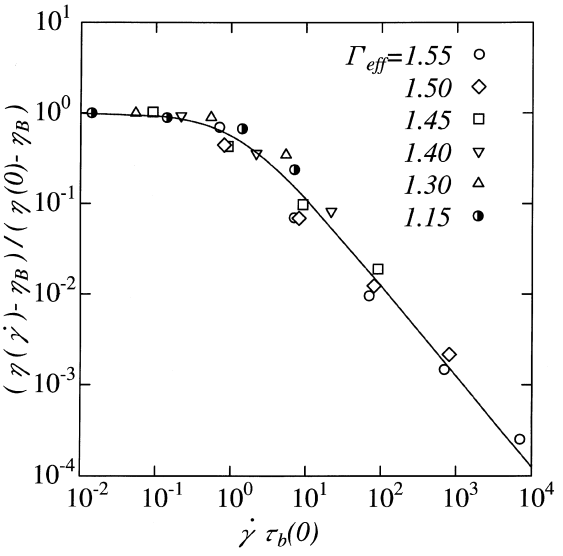

Fig. 10. $(\eta(\dot\gamma)-\eta_B)/(\eta(0)-\eta_B)$ versus $\dot\gamma\tau_b(0)$ in 3D.

We have also examined the transient behavior of the shear stress as a function of time after application of shear to find stress overshoots in glassy states in accord with the experiments. This aspect will be discussed in a forthcoming paper.

5. Concluding remarks

Most observations in this work remain unexplained. But they pose new problems and suggest new experiments. We make some comments below.

(1) The weakly bonded regions in Figs. 4 and 5 are purely dynamical objects. Such large scale heterogeneities cannot be found in snapshots of the densities, the stress tensor, the kinetic energy, etc. Important issues are then how they evolve in space and time and why they look so similar to the critical fluctuations in Ising systems.

(2) In our systems we have not yet detected essential differences between 2D and 3D except in the value of the dynamic exponent z.

(3) Our systems are highly compressed. In fact the volume fraction ϕ of the soft-core regions is 0.93 in 2D and 0.57 in 3D. Then even slight anisotropic changes of the pair correlation functions, $g_{\alpha\beta}(r)$, near the first peak ($\sim\sigma_{\alpha\beta}$) gives rise to the limiting shear stress $\sigma_{\rm lim}$, which is $\lesssim 5\%$ of the pressure in our case. On the other hand, in many fluid systems such as near-critical fluids or polymer solutions the structure factor of the composition can be anisotropic at long wavelengths when $\dot\gamma$ exceeds a small underlying relaxation rate [10].

(4) In our case there is no tendency of phase separation. However, there can be cases in which the composition fluctuations are increased towards glass transition temperatures. It is of great interest how the two transitions affect each other.

(5) Shear flow can induce composition fluctuation enhancement in asymmetric viscoelastic mixtures, when emergence of less viscous regions can reduce the effective viscosity [10]. This effect should come into play also in glassy states, for example, for large enough size ratios or in the presence of small attraction between the two components.

(6) The mechanism of the non-Newtonian behavior in supercooled liquids is new and should be further examined in experiments. For example, polymers should exhibit pronounced non-Newtonian behavior, as the glass transition is approached, even without entanglement.

(7) We assume that long range density fluctuations as observed by Fischer [20] are nonexistent in liquids composed of structureless particles. They

should originate from small density variations induced by nematic ordering of anisotropic molecules as revealed by a simulation [21] and as observed upon crystallization [22].

References

[1] J. Jäckle, Rep. Prog. Phys. 49 (1986) 171.
[2] M.D. Ediger, C.A. Angell, S.R. Nagel, J. Phys. Chem. 100 (1996) 13200.
[3] U. Bengtzelius, W. Götze, A. Sjölander, J. Phys. C 17 (1984) 5915.
[4] E. Leutheusser, Phys. Rev. A 29 (1984) 2765.
[5] G. Adam, J.H. Gibbs, J. Chem. Phys. 43 (1965) 139.
[6] M.H. Cohen, G.S. Grest, Phys. Rev. B 20 (1979) 1077.
[7] F.H. Stillinger, J. Chem. Phys. 89 (1988) 6461.
[8] M.M. Hurley, P. Harrowell, Phys. Rev. E 52 (1995) 1694; D.N. Perera, P. Harrowell, Phys. Rev. E 54 (1996) 1652.
[9] R. Yamamoto, A. Onuki, J. Phys. Soc. Jpn. 66 (1997) 2545.
[10] A. Onuki, J. Phys. C 9 (1997) 6119.
[11] J.H. Simmons, R.K. Mohr, C.J. Montrose, J. Appl. Phys. 53 (1982) 4075; J.H. Simmons, R. Ochoa, K.D. Simmons, J.J. Mills, J. Non-Cryst. Solids 105 (1988) 313.
[12] D. Richter, R. Frick, B. Farago, Phys. Rev. Lett. 61 (1988) 2465.
[13] R. Yamamoto, A. Onuki, Europhys. Lett. 40 (1997) 61.
[14] T. Muranaka, Y. Hiwatari, Phys. Rev. E 51 (1995) R2735; T. Muranaka, Y. Hiwatari, Prog. Theor. Phys. 126 (Suppl.) (1997) 403.
[15] J. Matsui, T. Odagaki, Y. Hiwatari, Phys. Rev. Lett. 73 (1994) 2452.
[16] D. Henderson, J.P. Leonard, in: D. Henderson (Ed.), Physical Chemistry, an Advanced Treatise, Academic Press, New York, 1971.
[17] B. Bernu, Y. Hiwatari, J.P. Hansen, J. Phys. C 18 (1985) L371.
[18] M.P. Allen, D.J. Tildesley, Computer Simulation of Liquids, Clarendon, Oxford, 1987.
[19] D.J. Evans, G.P. Morriss, Statistical Mechanics of Nonequilibrium Liquids, Academic Press, New York, 1990.
[20] E.W. Fischer, Physica A 201 (1993) 183.
[21] H. Weber, W. Paul, W. Kob, K. Binder, Phys. Rev. Lett. 78 (1997) 2136.
[22] M. Imai, K. Kaji, T. Kanaya, Phys. Rev. Lett. 71 (1993) 4162.